Coordinated prefrontal–hippocampal activity and navigation strategy-related prefrontal firing during spatial memory formation

Ignacio Negrón-Oyarzo[a,b], Nelson Espinosa[b], Marcelo Aguilar-Rivera[b,1], Marco Fuenzalida[a], Francisco Aboitiz[b], and Pablo Fuentealba[b,c,2]

[a]Instituto de Fisiología, and Centro de Neurobiología y Fisiopatología Integrativa, Facultad de Ciencias, Universidad de Valparaíso, 2340000 Valparaíso, Chile; [b]Centro Integrativo de Neurociencias y Departamento de Psiquiatría, Pontificia Universidad Católica de Chile, 8330024 Santiago, Chile; and [c]Centro de Investigación en Nanotecnología y Materiales Avanzados, Pontificia Universidad Católica de Chile, 7820436 Santiago, Chile

Edited by Terrence J. Sejnowski, Salk Institute for Biological Studies, La Jolla, CA, and approved May 31, 2018 (received for review November 21, 2017)

Learning the location of relevant places in the environment is crucial for survival. Such capacity is supported by a distributed network comprising the prefrontal cortex and hippocampus, yet it is not fully understood how these structures cooperate during spatial reference memory formation. Hence, we examined neural activity in the prefrontal–hippocampal circuit in mice during acquisition of spatial reference memory. We found that interregional oscillatory coupling increased with learning, specifically in the slow-gamma frequency (20 to 40 Hz) band during spatial navigation. In addition, mice used both spatial and nonspatial strategies to navigate and solve the task, yet prefrontal neuronal spiking and oscillatory phase coupling were selectively enhanced in the spatial navigation strategy. Lastly, a representation of the behavioral goal emerged in prefrontal spiking patterns exclusively in the spatial navigation strategy. These results suggest that reference memory formation is supported by enhanced cortical connectivity and evolving prefrontal spiking representations of behavioral goals.

prefrontal cortex | hippocampus | spatial reference memory | local field potential | spatial navigation

Spatial navigation allows animals to learn and remember the location of relevant locations, shaping, in the process, a spatial reference memory that is acquired over repeated exploration of relatively stable environmental conditions (1). During the acquisition of such memory, animals adjust their navigation patterns to optimize the path to the goal (2). To date, neural mechanisms underlying the acquisition of spatial reference memory are still under debate (3, 4).

It has been proposed that acquisition of spatial reference memory is supported by the interplay between the hippocampus and prefrontal cortex (5, 6). Indeed, hippocampal lesions impair acquisition and recall of spatial reference memory in rodents (7–9) and humans (10, 11). On the other hand, the prefrontal cortex, which is involved in flexible and adaptive accommodation of goal-directed behavioral responses (12, 13), may provide the selection of the optimal trajectory to the goal. In agreement with this idea, lesions of the prefrontal cortex in humans (14) and its rodent analog, the medial prefrontal cortex (15), impair the implementation of the optimal navigation strategy in spatial reference navigation tasks (16–18). Prefrontal neurons encode a wide range of behaviorally relevant aspects, including decision making, goal location, strategy switch, and reward approach during spatial working-memory tasks (19–21). Such diversity of computations might be related with the integration of different types of information required for the implementation of the optimal path to the goal. Importantly, the prefrontal cortex exhibits strong anatomical connectivity with the hippocampus (22, 23). Thus, current thinking suggests that acquisition of spatial reference memory is supported by distributed neural systems, with the hippocampus communicating the animal's current position in the environment (24, 25) to the prefrontal cortex, which in turn uses such information for the optimization of navigation routes to the goal (4–6, 26). To date, it is not completely known how the prefrontal cortex may represent behaviorally relevant information during spatial reference memory formation.

Increasing evidence suggests that communication between neural systems is supported by synchronization of oscillatory activity (27, 28). We hypothesize that synchrony between the prefrontal cortex and hippocampus might support acquisition of spatial reference memory. Here, we report that the acquisition of reference memory in the Barnes maze was associated with changes in oscillatory synchrony of the prefrontal–hippocampal circuit, together with modifications in the related spike timing of prefrontal cortex neurons as well as changes in firing activity, and the neural representation of the behavioral goal (i.e., entering the escape hole) in spiking patterns of the prefrontal cortex. These results support the role of the prefrontal–hippocampal network in the acquisition of spatial reference memory and show a differential recruitment of prefrontal cortical activity depending on the type of implemented navigation strategy.

Significance

Learning the location of relevant places is an iterative process in which animals gradually adjust and optimize their navigation patterns to reach the target. This cognitive operation requires the interplay between the hippocampus, which represents the animal's current location, and the prefrontal cortex, which implements the selection of adaptive behavioral responses. Yet, how do these structures interact during spatial learning? By recording neural activity in freely behaving mice, we found that the prefrontal cortex and hippocampus gradually increase their oscillatory synchrony as learning progresses, whereas the firing patterns of prefrontal neurons represent the behavioral goal exclusively when the optimal trajectory is selected. These findings provide insight into the cortical dynamics underlying spatial learning.

Author contributions: I.N.-O., F.A., and P.F. designed research; I.N.-O. performed research; N.E., M.A.-R., and M.F. contributed new reagents/analytic tools; I.N.-O. and N.E. analyzed data; and I.N.-O. and P.F. wrote the paper.

The authors declare no conflict of interest.

This article is a PNAS Direct Submission.

[1]Present address: Department of Bioengineering, University of California, San Diego, La Jolla, CA 92093.

[2]To whom correspondence should be addressed. Email: pfuentealba@uc.cl.

This article contains supporting information online at www.pnas.org/lookup/suppl/doi:10.1073/pnas.1720117115/-/DCSupplemental.

Published online June 18, 2018.

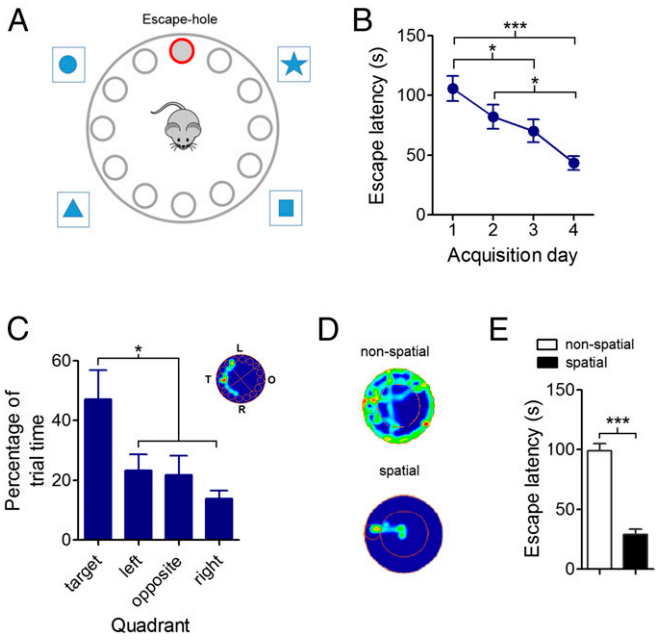

Fig. 1. Behavioral performance and navigation strategies during acquisition of spatial reference memory in the Barnes maze. (*A*) Schematic diagram of the Barnes maze. Mice learn to escape from an aversive (open, illuminated, and elevated) environment by following spatial cues and locating an escape hole. After several navigation trials, mice learn the location of the escape hole. (*B*) Average escape latency per day during acquisition (***$P <$ 0.0001, *$P <$ 0.05; Bonferroni's multiple comparison test after one-way ANOVA; n = 10 animals, 149 trials). Data are presented as mean ± SEM. (*C*) Bar charts of proportion of time spent on each quadrant during the probe trial (*$P <$ 0.05; Bonferroni's multiple comparison test after one-way ANOVA; n = 9 animals, 9 trials). (*Inset*) Example of occupancy plot during a probe trial (warm colors denote longer occupancy times, whereas cold colors indicate shorter occupancy times). Data are presented as mean ± SEM. L, left; O, opposite; R, right; T, target. (*D*) Examples of occupancy plots for nonspatial and spatial navigation strategies. Warm colors denote longer occupancy times, whereas cold colors indicate shorter occupancy times. (*E*) Bar chart of escape latency for nonspatial and spatial navigation strategies (***$P <$ 0.0001; Student t test; n = 10 animals, 149 trials). Data are presented as mean ± SEM.

Results

Behavioral Performance and Navigation Strategies During Reference Memory Formation. Mice were trained in the Barnes maze, a spatial reference memory task (29) in which mice learn the location of an escape hole after several exploration trials (Fig. 1*A*). Animals correctly learned the task, as their escape latency progressively decreased over time ($P <$ 0.0001, Fig. 1*B* and *SI Appendix*, Fig. S1*A*). Similarly, the number of errors significantly decreased across days ($P <$ 0.0001, *SI Appendix*, Fig. S1*B*), with no significant changes in either maximum or average speed (P = 0.197, *SI Appendix*, Fig. S1 *C* and *D*). After training was completed, a spatial reference memory was formed, as we found significant differences in exploration times of quadrants in the probe test (P = 0.0082, Fig. 1*C*), with mice spending significantly more time in the target quadrant compared with the other quadrants ($P <$ 0.05). Mice implemented two types of navigation strategy to reach the target: a nonspatial strategy, in which spatial cues were not used to locate the escape hole; and a spatial strategy that exploited distal cues and exhibited a direct trajectory to the escape quadrant (Fig. 1*D* and Movies S1–S3) (30, 31). As learning progressed, the use of the spatial strategy increased (*SI Appendix*, Fig. S1*E*). Navigation time was minimized by the spatial strategy, as escape latency was significantly shorter ($P <$ 0.0001, Fig. 1*E*) and the number of errors was significantly lower ($P <$ 0.0001, *SI Appendix*, Fig. S1*F*) compared with the nonspatial strategy. By definition, the spatial strategy also minimized the traveled distance to reach the escape hole (P = 0.013, *SI Appendix*, Fig. S1*G*). Importantly, there were no significant differences between strategies in either the maximum or average speed of navigation ($P >$ 0.05, *SI Appendix*, Fig. S1 *H* and *I*). Altogether, these data suggest that animals progressively learned to solve the task, generating a spatial reference memory of the escape hole. During this process, mice displayed two broad types of navigation strategy, of which the spatial strategy was the most efficient to solve the task.

Evolution of Prefrontal–Hippocampal Connectivity During Learning. Synchronization of neural oscillations has been proposed as a mechanism for functional coupling of distributed neural systems (30, 31). Therefore, we asked whether local field potential (LFP) spectral coherence in the prefrontal–hippocampal circuit was modulated by task acquisition. We identified elevated interregional coherence in theta (6 to 10 Hz) oscillations during spatial navigation (Fig. 2 *A* and *B* and *SI Appendix*, Fig. S2*B*) (20, 32), which did not change during task acquisition (P = 0.381, Fig. 2 *B* and *C*). Importantly, we found prominent coherence in the slow-gamma band (20 to 40 Hz; Fig. 2 *A* and *B*), which progressively increased over time with task acquisition (P = 0.002, Fig. 2 *B* and *D* and *SI Appendix*, Fig. S2*B*); however, the fast-gamma band (60 to 80 Hz) showed no significant changes over time (P = 0.488, Fig. 2*E*). Moreover, we did not identify changes in oscillatory coupling in any frequency band over time when recording animals freely moving in the home cage (theta: P = 0.149; slow-gamma: P = 0.650; fast-gamma: P = 0.492, *SI Appendix*, Fig. S2*C*), suggesting that increased coherence was specific to the behavioral task. Next, we tested whether enhanced coherence was specific to some particular phase of the task. For this, we divided each trial into three phases: start, navigation, and goal (see *Materials and Methods*). Indeed, peaks of enhanced coherence were selectively detected in the navigation phase for both the theta and slow-gamma bands (*SI Appendix*, Fig. S2*D*). Importantly, time-evolving cortical coherence during navigation could be impacted by potential changes in locomotor patterns of

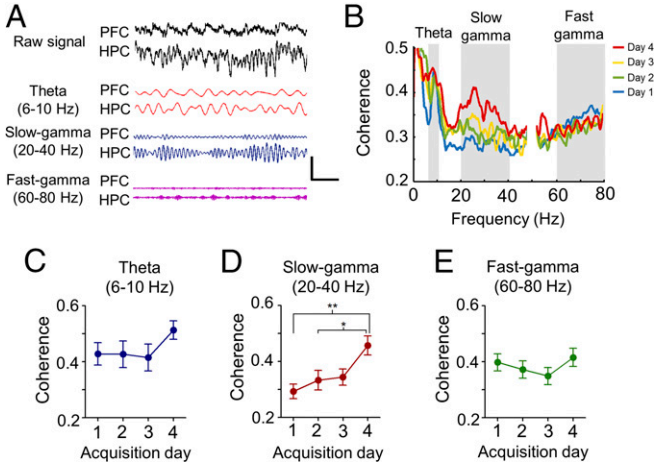

Fig. 2. Synchronous activity between prefrontal cortex and hippocampus during acquisition of spatial reference memory. (*A*) Examples of simultaneous LFP traces recorded from the prefrontal cortex (PFC) and hippocampus (HPC), and filtered at theta, slow-gamma, and fast-gamma frequency bands (calibration bar: 250 μV, 500 ms; mouse code: IN67). (*B*) Mean prefrontal–hippocampus coherence as a function of frequency across acquisition days (n = 7 animals, 99 trials). (*C*–*E*) Mean PFC-HPC coherence across acquisition days at theta (*C*), slow-gamma (*D*) and fast-gamma (*E*) frequency bands (*$P <$ 0.05; **$P <$ 0.01; Bonferroni's multiple comparison test after one-way ANOVA). Data are presented as mean ± SEM.

mice taking place during learning, and not be exclusively related to enhanced cortical connectivity subserving task acquisition. To control for this possibility, we refined our analysis of movement patterns to assess the influence of running speed and LFP oscillatory variability on cortical coupling (*Materials and Methods*). This analysis showed the lack of dependence between cortical connectivity and movement patterns, suggesting that enhanced cortical connectivity as defined by spectral coherence is unlikely to result from broad changes of mice locomotor behavior (*SI Appendix*, Figs. S3 and S4). Overall, these data suggest that learning was associated with the progressive enhancement of prefrontal–hippocampal coupling in the slow-gamma frequency band specifically during navigation.

Increased interregional coherence may result from changes in the amplitude of oscillatory activity or enhanced phase coupling (33, 34) Indeed, we found significant differences specifically in the power of prefrontal theta activity ($P = 0.0067$, *SI Appendix*, Fig. S5 *B* and *C*) and slow-gamma activity across acquisition days ($P = 0.019$; *SI Appendix*, Fig. S5 *B* and *C*). We detected no association between hippocampal spectral power and acquisition day in the theta or slow-gamma bands (theta: $P = 0.089$; slow-gamma: $P = 0.231$; *SI Appendix*, Fig. S5 *E* and *F*). No changes throughout acquisition were detected in the fast-gamma band, in prefrontal cortex ($P = 0.631$; *SI Appendix*, Fig. S5 *B* and *C*), or hippocampus ($P = 0.905$; *SI Appendix*, Fig. S5 *E* and *F*). In addition to acquisition day, increased spectral power in the prefrontal cortex, but not the hippocampus, was also dependent on the phase of the task ($P = 0.0055$), taking place specifically during the navigation phase (*SI Appendix*, Fig. S5*G*), consistent with enhanced coherence occurring during the same phase. Hence, these results suggest that enhanced prefrontal–hippocampal coupling during learning was mainly the result of increased amplitude of prefrontal cortical rhythms.

Rhythmic Synchronization and Prefrontal Spiking of Prefrontal Neurons During Navigation. Cortical oscillations synchronize neuronal spiking, thus contributing to the temporal integration of neural activity (27). Therefore, we asked whether cortical rhythms modulated the spike timing of prefrontal neurons in relation to task acquisition. Hence, we recorded spiking activity from the prefrontal cortex (*SI Appendix*, Fig. S6 and Tables S1 and S2). As a population, prefrontal neurons did not discharge in relation to a particular frequency band (*SI Appendix*, Fig. S7*A*). However, groups of cells were significantly modulated by theta or slow-gamma oscillations (34.6% and 17.8% of prefrontal units, respectively; Fig. 3 *C* and *F*). Phase-locking strength did not vary across days during task acquisition (theta: $P = 0.461$; slow-gamma: $P = 0.377$; *SI Appendix*, Fig. S7 *B* and *C*). However, phase locking was larger for the spatial strategy compared with the nonspatial strategy, for both local theta oscillations ($P = 0.013$, *SI Appendix*, Fig. S7*D*) and slow-gamma oscillations ($P = 0.010$, *SI Appendix*, Fig. S7*E*). Importantly, these differences were specifically detected during the navigation phase of the task (theta: $P = 0.012$, slow-gamma: $P = 0.0006$; Fig. 3 *D* and *G*), as there were no significant differences in the start or goal phases of the task in phase locking for either theta oscillations (start: $P = 0.189$, goal: $P = 0.258$; Fig. 3*D*) or slow-gamma oscillations (start: $P = 0.783$, goal: $P = 0.279$; Fig. 3*G*). Moreover, phase locking was cell type specific, as only regular-spiking units were modulated by navigation strategy, whereas fast-spiking units were not. Such was the case for both theta oscillations (regular spiking: $P = 0.0036$; fast spiking: $P = 0.542$; *SI Appendix*, Fig. S7*F*) and slow-gamma oscillations (regular spiking: $P = 0.0006$; fast spiking: $P = 0.500$; *SI Appendix*, Fig. S7*G*). Importantly, phase-locking strength of prefrontal units in both frequency bands was significantly correlated with escape latency (theta: $r = -0.39$, $P < 0.0001$; slow-gamma: $r = -0.43$, $P < 0.0001$; Fig. 3 *E* and *H*).

Hippocampal oscillations also modulated a sizable proportion of prefrontal cells (theta oscillations, 30.3%; slow-gamma

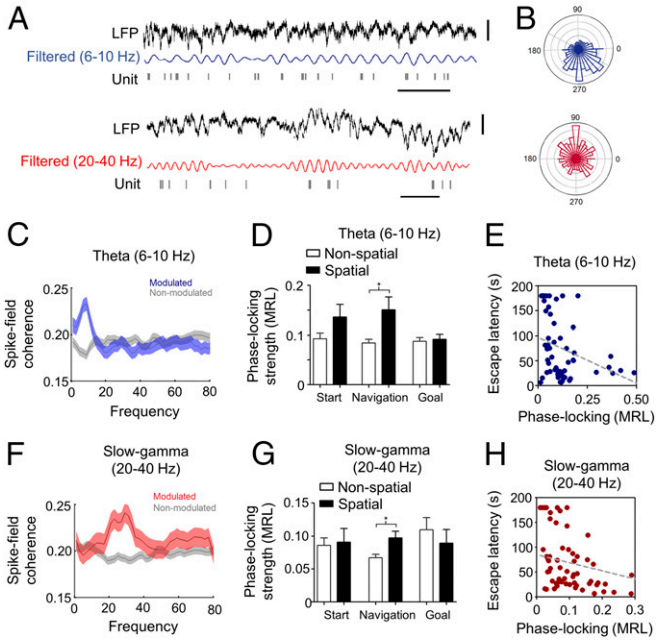

Fig. 3. Modulation of neuronal spiking in the prefrontal cortex by cortical oscillations and navigation strategy. (*A*) Examples of theta-modulated and slow-gamma–modulated prefrontal units. (*Top*) LFP (black) and theta-filtered (blue) prefrontal LFP recording, along with simultaneous raster plot of prefrontal single-unit activity (gray). (*Bottom*) Same as above, but for a prefrontal single unit modulated by local slow-gamma oscillation. (*B*) Phase histogram of phase preference for units showed in *A*, same color code. (*Top*) Example unit modulated by theta oscillation [$P = 2.87 \times 10^{-5}$, ln(Z) = 2.34; mean resultant length (MRL) = 0.126; Rayleigh test for circular uniformity]. (*Bottom*) Example unit modulated by slow-gamma oscillation [$P = 5.9 \times 10^{-34}$, ln(Z) = 4.31; MRL = 0.338; Rayleigh test for circular uniformity]. (*C* and *F*) Mean spike-field coherence of all significantly modulated (blue or red; $n = 64$ units for theta; 33 units for slow-gamma) and nonmodulated (gray; $n = 121$ units for theta; 151 units for slow-gamma) prefrontal units by local theta (*C*) or slow-gamma (*F*) oscillations. Shading areas depict SEM. (*D* and *G*) Bar charts of phase-locking strength (MRL) of prefrontal units to local theta (*D*) and slow-gamma oscillations (*G*) for navigation strategies during different task phases (*$P < 0.05$; Mann–Whitney *U* test). (*E* and *H*) Correlation between trial-averaged escape latency and trial-averaged phase-locking strength of regular-spiking units to local theta (*E*) ($P < 0.001$; $r = -0.38$, Spearman correlation analysis) or slow-gamma oscillations (*H*) ($P < 0.001$; $r = -0.42$, Spearman correlation analysis) during the navigation phase.

oscillations, 13.5%; *SI Appendix*, Fig. S7 *D* and *E*). Their phase locking to hippocampal oscillations did not vary over time during task acquisition (theta: $P = 0.929$, slow-gamma: $P = 0.377$; *SI Appendix*, Fig. S7 *J* and *K*) but it was navigation strategy dependent for theta oscillations ($P = 0.0057$, *SI Appendix*, Fig. S7*H*), in agreement with our findings in prefrontal cortical oscillations. However, phase locking was not different for hippocampal slow-gamma oscillations ($P = 0.051$, *SI Appendix*, Fig. S7*I*).

We next evaluated changes in neuronal firing activity in the prefrontal cortex during task acquisition. Cortical spiking rates were not different across conditions (*SI Appendix*, Fig. S8). However, when normalized by the mean firing rate, activity was larger for the spatial strategy compared with the nonspatial strategy (Fig. 4 *A* and *B*), specifically for the navigation phase of the task ($P = 0.036$, Fig. 4*C*). Interestingly, differences were not seemingly related to the temporal evolution of learning, as normalized prefrontal activity during task acquisition showed no significant differences over time (*SI Appendix*, Fig. S9). Differences in neuronal activity between navigation strategies were cell type specific, as they were detected only in regular-spiking units

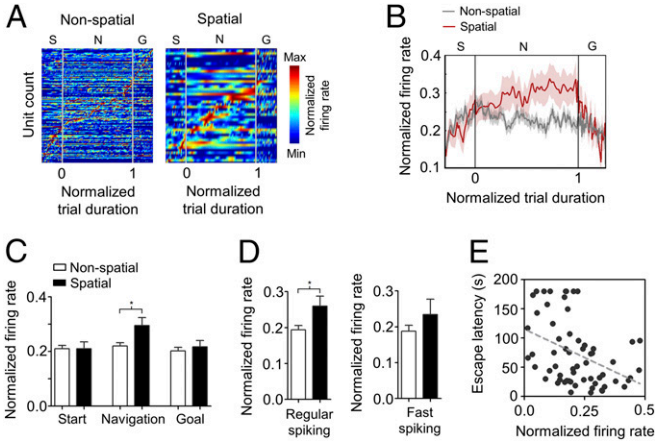

Fig. 4. Dynamics of prefrontal cortex firing patterns during spatial navigation. (*A*) Color-coded firing patterns of single units recorded in the prefrontal cortex during nonspatial (*Left*) and spatial (*Right*) navigation strategies. Each row represents the color-coded normalized firing rate of one unit (nonspatial, $n = 180$ units; spatial, $n = 47$ units) sorted by the timing of peak firing rate. Task-relevant events—navigation onset and escape hole entering—are indicated as points 0.0 and 1.0, respectively. Start (S) and goal (G) phases had fixed durations of 1 min each. The navigation (N) phase varied between 7 and 180 s (median = 57.4 s) but was normalized by number of bins. (*B*) Temporal evolution of average normalized firing rate during the complete task for nonspatial and spatial navigation strategies. Shaded areas depict SEM. (*C*) Bar chart of mean normalized firing rates for navigation strategies and phase of the task (*$P < 0.05$; Mann–Whitney *U* test). Data are presented as mean ± SEM. (*D*) Bar chart of mean normalized firing rate between navigation strategies for regular-spiking (*Left*) and fast-spiking units (*Right*) (*$P < 0.05$; Mann–Whitney *U* test). (*E*) Correlation between trial-averaged normalized firing rate of regular-spiking units during the navigation phase and trial-averaged escape latency ($P = 0.0011$; $r = -0.165$, Spearman correlation analysis).

($P = 0.045$, Fig. 4*D*). Lastly, we found that normalized firing activity correlated with escape latency (Fig. 4*E*). These results reveal that phase locking of prefrontal principal neurons to local oscillations, as well as firing activity, increased during learning as spatial navigation developed specifically during the navigation phase of the task and correlated with behavioral performance.

Neural Representation of the Behavioral Goal. During spatial navigation, the occurrence of task-relevant events is represented in prefrontal neurons by changes in their firing patterns (19, 20, 35, 36). Therefore, we sought to identify such neural representations, in particular the escape hole, which denotes the goal of the current navigation task (Fig. 5*A*). On average, spiking activity in the prefrontal cortex did not vary when animals reached the escape hole (*SI Appendix*, Fig. S10*B*). However, when focusing on the spatial strategy, prefrontal neurons selectively increased their activity briefly before animals entered the escape hole ($P < 0.05$, Fig. 5*B*). Interestingly, we did not find significant changes in firing activity correlated to a nose poke in the escape hole when the mouse did not step into it (Fig. 5 *C* and *D*), discarding an exclusive representation of the goal's location. Moreover, increased discharge probability was exclusive to the escape hole, as we did not detect significant changes in firing in nonescape holes (i.e., errors, *SI Appendix*, Fig. S10 *C* and *D*). Altogether, these results suggest that prefrontal units encode a representation of the behavioral goal specifically during the spatial navigation strategy.

We also estimated neuronal selectivity for the behavioral goal (i.e., entering the escape hole) by calculating the biased-firing index for the escape hole (*Materials and Methods*). We found that firing selectivity to the action of escape was indeed dependent on the type of navigation strategy implemented, as prefrontal neurons had a larger mean firing bias for entering the escape hole in the spatial strategy compared with nonspatial navigation ($P = 0.0031$, Fig. 5*E*). No changes in firing selectivity for the escape hole were detected across acquisition days ($P = 0.232$, *SI Appendix*, Fig. S10*E*). Furthermore, differences in selectivity to the escape hole between navigation strategies were cell type specific, as regular-spiking units showed significant differences between navigation strategies ($P = 0.001$, Fig. 5*F*). Furthermore, we found that the spatial selectivity index of regular-spiking prefrontal neurons was significantly correlated with the escape latency ($r = -0.175$, $P = 0.004$; Fig. 5*G*). Lastly, we compared firing selectivity to nose poking in the escape hole between

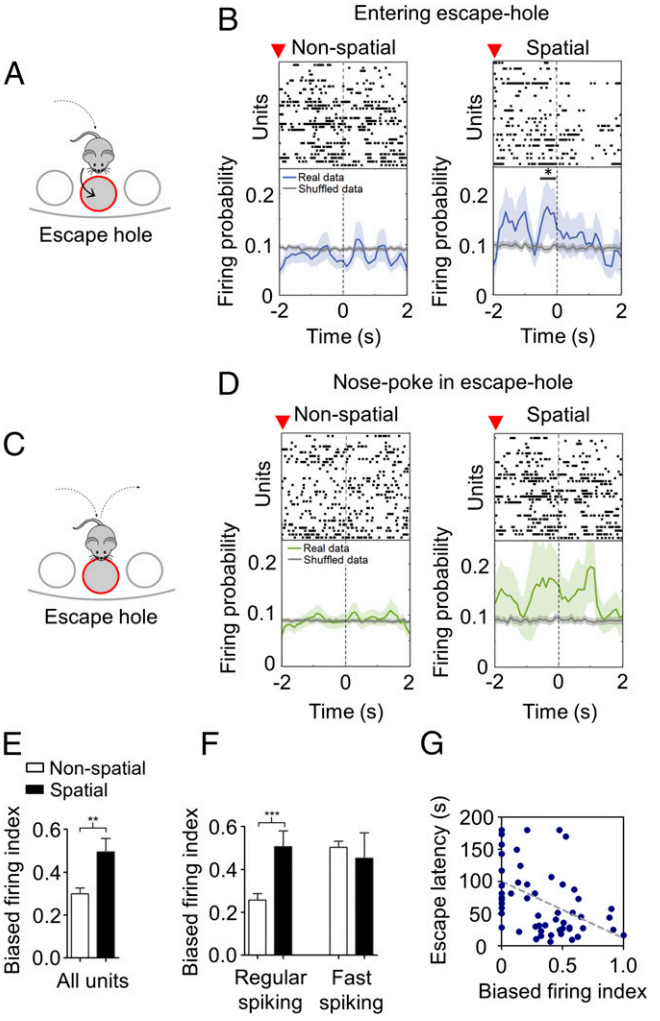

Fig. 5. Neural representation of task-relevant events in the spike timing of prefrontal units. (*A* and *C*) Schematic diagram of task-relevant events: entering (*A*) or nose poking into (*C*) the escape hole. (*B* and *D*) Example raster plots and average normalized peri-event time histograms of prefrontal units firing during nonspatial and spatial navigation strategies aligned at the time when the mouse either enters (*B*) or nose pokes into (*D*) the escape hole. Shuffled data are also displayed (gray line). Superior red arrow indicates time at which mice are at 4 cm from the escape hole. Shading areas indicate SEM (*$P < 0.05$ with respect to shuffled data, paired Wilcoxon signed-rank test). (*E*) Bar chart comparing mean biased firing index for the escape hole for all units across navigation strategies (**$P < 0.01$; Mann–Whitney *U* test). Data are presented as mean ± SEM. (*F*) Same as *E*, but for regular- and fast-spiking units (***$P < 0.001$; Mann–Whitney *U* test). Data are presented as mean ± SEM. (*G*) Correlation between trial-averaged escape latency and trial-averaged biased-firing index of regular-spiking units ($P = 0.0044$; $r = -0.175$, Spearman correlation analysis).

navigation strategies and found no significant differences ($P = 0.086$, *SI Appendix*, Fig. S10*F*). In addition, the temporal evolution of task acquisition did not show a significant relation with nose-poking firing selectivity ($P = 0.999$, *SI Appendix*, Fig. S10*E*). Moreover, we did not find significant differences in nose-poking firing selectivity between navigation strategies in regular-spiking ($P = 0.076$) or fast-spiking units ($P = 0.941$, *SI Appendix*, Fig. S10*G*). Overall, these data suggest that prefrontal principal neurons encode the escape action, rather than the location of the escape hole, by briefly increasing their discharge probability specifically during the spatial navigation strategy.

Discussion

Our results show that learning the spatial location of goals was associated with increased prefrontal–hippocampal functional connectivity, as well as with increased phase locking, firing activity, and encoding of behavioral goals by prefrontal neurons. Importantly, these changes observed in prefrontal neuronal activity were associated with the implementation of the most efficient navigation strategy during learning.

The implementation of optimal navigation strategies depends on the integration of environmental signals comprising both spatial and nonspatial cues (31). In the current study, utilization of the spatial strategy progressively increased over time, reflecting the gradual adjustment of navigation patterns to minimize the path to the goal (2). This may indicate that spatial information was not immediately incorporated into navigation pattern. Instead, it was gradually integrated across exploration trials. Since topological representation of the environment (i.e., the cognitive map) is generated in a single trial (37, 38) and optimal navigation patterns evolve gradually during the task, we suggest that spatial information is slowly incorporated into the optimal behavioral response. Thus, different reference frames, such as place- and response-based reference frames, may cooperate during the implementation of the optimal path to the goal (39). The place-based reference frame involves a topological representation of the environment, whereas the response-based reference frame stores the rules of the task, which encompasses the association between sensory cues (i.e., reward associated to the goal) and behavior (i.e., navigation in the environment). The independence from the subject's orientation observed in the spatial strategy is a characteristic of place-reference learning (2), whereas the slow acquisition rate under landmark stability is a distinctive feature of response-based learning (40), supporting the progressive cooperation of both reference systems. Indeed, lesion studies have shown that both reference frames depend on distinct neural systems (41, 42), in which place-based navigation relies on the hippocampus (39, 43) and response-based navigation depends on the prefrontal cortex (18, 43, 44). Therefore, this suggests that the implementation of the optimal route to the target requires the interplay between distributed neural circuits. In this model, the hippocampus enacts the place-based reference frame, whereas the prefrontal cortex executes the response-based reference frame (4).

We hypothesized that the interplay between prefrontal cortex and hippocampus required for the acquisition of reference memory is supported by gradual synchronization. We observed that coherence in the theta band was stable over time or between navigation strategies, suggesting that, at least in the current task, it was not related to learning. Previous results in rodents suggest that hippocampal slow-gamma oscillations may encode novel environments (45–47). Moreover, slow-gamma oscillations in the primate prefrontal cortex increase with cognitive effort (48–50) and seem to be involved in higher-order executive functioning such as rule selection (51). Therefore, it has been proposed that power increments in slow-gamma oscillations are associated with the active maintenance of the current cognitive set during strong endogenous top-down processing (52). Thus, the emergence of slow-gamma synchrony may help to maintain and associate distributed information to achieve a behavioral goal during spatial navigation. These results point to slow-gamma coupling in the prefrontal–hippocampal network as a potential mechanism for linking activity across distributed cortical regions in reference memory formation.

We found that during task acquisition, both local theta and slow-gamma oscillations modulated the spike timing of prefrontal neurons, which increased in relation to the utilization of the spatial strategy and correlated with behavioral performance. These results are in agreement with previous reports in which both prefrontal and hippocampal theta oscillations modulated the spike timing of prefrontal neurons (32, 53). Similarly, it has been shown that primate prefrontal neurons showed increased phase locking to local slow-gamma in a rule-dependent way (51). Likewise, there is a learning-dependent increase in phase locking of cortical neurons to hippocampal and entorhinal slow-gamma oscillations (54). Altogether, these data suggest that phase locking of prefrontal pyramidal neurons to both prefrontal and hippocampal oscillations is a neural mechanism favored by the spatial navigation strategy, which probably relates to path optimization during reference memory formation.

Our results show that during reference memory formation, pyramidal prefrontal neurons are selectively modulated by the navigation strategy in at least two ways and in different temporal scales. Indeed, during the implementation of the spatial strategy, principal cortical neurons progressively increased their activity (during seconds) as the animal approached the target (i.e., escape hole). This is not related to changes in running speed, as we found that individual movement episodes were, in fact, slower for the spatial strategy compared with the nonspatial strategy. In addition to the previous pattern, pyramidal cells signaled the goal action just before engagement. In fact, cortical neurons selectively increased their firing rate for a brief period (<1 s) just before stepping into the escape hole. Possibly, this correlated, increased activity signals the animal's commitment to the motor action of entering the escape hole. Further experiments will have to test this idea. The absence of changes in firing activity inside the escape hole, as well as during nose poking into either escape or nonescape holes, suggests that prefrontal neurons do not represent the target (i.e., escape hole), the maze holes, or target approaching. Therefore, these results suggest that in the spatial navigation strategy, a representation of the behavioral goal (i.e., entering the escape hole) emerges in prefrontal spiking patterns. These findings are consistent with previous reports showing behavioral prediction by prefrontal neurons as (*i*) directional goal choice in working-memory tasks (19, 21, 55), (*ii*) exploration of aversive environments in the elevated plus-maze (56), and (*iii*) strategy switching (57). Altogether, these data support the role of prefrontal neurons in guiding and implementing adaptive behavior by encoding behavioral goals.

Overall, we have shown that behavioral changes in navigation patterns during reference memory formation are accompanied by modifications in functional connectivity in the prefrontal–hippocampal network, as well as changes in oscillatory coupling, activity, and selectivity of prefrontal neurons. Altogether, our results provide insight into the dynamics of the prefrontal–hippocampal network during reference memory formation in a spatial navigation task.

Materials and Methods

Ten adult male C57BL/6j mice were implanted with custom-made microdrives carrying three tetrodes targeting the medial prefrontal cortex (1.94 mm anteroposterior, 0.5 mm mediolateral from bregma) and one tetrode targeting the dorsal CA1 hippocampus (−1.54 mm anterior, 1.5 mm lateral from bregma). After recovery from surgery, mice were trained in the Barnes maze task, as previously described (29). On each session, mice explored an open, illuminated, and elevated circular platform limited by 16 equidistant holes, in which one of them, located in a fixed position, was the escape hole of the

maze. Each mouse performed four trials per day during 4 consecutive days. In each training session, prefrontal (single units and LFP) and hippocampus (LFP) activity was simultaneously recorded. Maze navigation was monitored and video-tracked throughout training sessions, and data were stored for posterior offline analysis. Behavioral analysis included quantification of escape latency, number of errors (nose poke in nonescape holes), and classification of navigation strategy, as previously described (31). Spectral analysis of LFP coherence and power were computed using multitaper Fourier analysis from the Chronux toolbox (chronux.org/home/) by using MATLAB. Spike sorting was performed offline using MATLAB-based graphical cluster-cutting software, Mclust/Klustakwik-toolbox (version 3.5; ref. 58). Spike-field coherence was computed using the multitaper Fourier analysis (34) and the Chronux toolbox (chronux.org/home/), and phase-locking analysis was computed using the MATLAB toolbox CircStats. To verify recording sites, Nissl-staining was conducted after the completion of study. See *SI Appendix, SI Materials and Methods* for a detailed description of the experimental and analytic methods.

ACKNOWLEDGMENTS. We thank Maria José Díaz and Marcelo Stockle for their technical assistance and Dr. Daniel Rojas and Dr. Sebastian Fuentes for commenting on previous versions of the manuscript. This work was funded by a Millennium Center for the Neuroscience of Memory Grant (NC10-001-F) from the Ministry of Economy, Development and Tourism, Chile; a Fondecyt Regular Grant (1141089) from the National Commission for Scientific and Technological Research (CONICYT), Chile (to P.F.); a Fondecyt Postdoctoral Grant (3140370) and a Fondecyt for Initiation into Research Grant (11160251) from CONICYT, Chile (to I.N.-O.); and Programa de Investigacion Asociativa (PIA) Anillos de Ciencia y Tecnologia (ACT) 1414.

1. Prior H, Schwegler H, Dücker G (1997) Dissociation of spatial reference memory, spatial working memory, and hippocampal mossy fiber distribution in two rat strains differing in emotionality. *Behav Brain Res* 87:183–194.
2. O'Keefe J, Nadel L (1978) *The Hippocampus as a Cognitive Map* (Oxford Univ Press, Oxford).
3. Poucet B, et al. (2015) Is there a pilot in the brain? Contribution of the self-positioning system to spatial navigation. *Front Behav Neurosci* 9:292.
4. Poucet B, Hok V (2017) Remembering goal locations. *Curr Opin Behav Sci* 17:51–56.
5. Poucet B, et al. (2004) Spatial navigation and hippocampal place cell firing: The problem of goal encoding. *Rev Neurosci* 15:89–107.
6. Spiers HJ, Gilbert SJ (2015) Solving the detour problem in navigation: A model of prefrontal and hippocampal interactions. *Front Hum Neurosci* 9:125.
7. O'Keefe J, Nadel L, Keightley S, Kill D (1975) Fornix lesions selectively abolish place learning in the rat. *Exp Neurol* 48:152–166.
8. Morris RG, Garrud P, Rawlins JN, O'Keefe J (1982) Place navigation impaired in rats with hippocampal lesions. *Nature* 297:681–683.
9. Sloan HL, Good M, Dunnett SB (2006) Double dissociation between hippocampal and prefrontal lesions on an operant delayed matching task and a water maze reference memory task. *Behav Brain Res* 171:116–126.
10. Rosenbaum RS, et al. (2000) Remote spatial memory in an amnesic person with extensive bilateral hippocampal lesions. *Nat Neurosci* 3:1044–1048.
11. Kessels RP, de Haan EH, Kappelle LJ, Postma A (2001) Varieties of human spatial memory: A meta-analysis on the effects of hippocampal lesions. *Brain Res Brain Res Rev* 35:295–303.
12. Fuster JM (2001) The prefrontal cortex—An update: Time is of the essence. *Neuron* 30:319–333.
13. Miller EK, Cohen JD (2001) An integrative theory of prefrontal cortex function. *Annu Rev Neurosci* 24:167–202.
14. Ciaramelli E (2008) The role of ventromedial prefrontal cortex in navigation: A case of impaired wayfinding and rehabilitation. *Neuropsychologia* 46:2099–2105.
15. Uylings HBM, Groenewegen HJ, Kolb B (2003) Do rats have a prefrontal cortex? *Behav Brain Res* 146:3–17.
16. Sutherland RJ, Whishaw IQ, Kolb B (1988) Contributions of cingulate cortex to two forms of spatial learning and memory. *J Neurosci* 8:1863–1872.
17. Kolb B, Buhrmann K, McDonald R, Sutherland RJ (1994) Dissociation of the medial prefrontal, posterior parietal, and posterior temporal cortex for spatial navigation and recognition memory in the rat. *Cereb Cortex* 4:664–680.
18. Ethier K, Le Marec N, Rompré PP, Godbout R (2001) Spatial strategy elaboration in egocentric and allocentric tasks following medial prefrontal cortex lesions in the rat. *Brain Cogn* 46:134–135.
19. Fujisawa S, Amarasingham A, Harrison MT, Buzsáki G (2008) Behavior-dependent short-term assembly dynamics in the medial prefrontal cortex. *Nat Neurosci* 11:823–833.
20. Benchenane K, et al. (2010) Coherent theta oscillations and reorganization of spike timing in the hippocampal-prefrontal network upon learning. *Neuron* 66:921–936.
21. Ito HT, Zhang S-J, Witter MP, Moser EI, Moser M-B (2015) A prefrontal-thalamo-hippocampal circuit for goal-directed spatial navigation. *Nature* 522:50–55.
22. Swanson LW (1981) A direct projection from Ammon's horn to prefrontal cortex in the rat. *Brain Res* 217:150–154.
23. Jay TM, Witter MP (1991) Distribution of hippocampal CA1 and subicular efferents in the prefrontal cortex of the rat studied by means of anterograde transport of Phaseolus vulgaris-leucoagglutinin. *J Comp Neurol* 313:574–586.
24. Buzsáki G (2005) Theta rhythm of navigation: Link between path integration and landmark navigation, episodic and semantic memory. *Hippocampus* 15:827–840.
25. Buzsáki G, Moser EI (2013) Memory, navigation and theta rhythm in the hippocampal-entorhinal system. *Nat Neurosci* 16:130–138.
26. Spiers HJ, Maguire EA (2007) The neuroscience of remote spatial memory: A tale of two cities. *Neuroscience* 149:7–27.
27. Fell J, Axmacher N (2011) The role of phase synchronization in memory processes. *Nat Rev Neurosci* 12:105–118.
28. Varela F, Lachaux JP, Rodriguez E, Martinerie J (2001) The brainweb: Phase synchronization and large-scale integration. *Nat Rev Neurosci* 2:229–239.
29. Negron-Oyarzo I, Neira D, Espinosa N, Fuentealba P, Aboitiz F (2015) Prenatal stress produces persistence of remote memory and disrupts functional connectivity in the hippocampal-prefrontal cortex axis. *Cereb Cortex* 25:3132–3143.
30. Koopmans G, Blokland A, van Nieuwenhuijzen P, Prickaerts J (2003) Assessment of spatial learning abilities of mice in a new circular maze. *Physiol Behav* 79:683–693.
31. Harrison FE, Reiserer RS, Tomarken AJ, McDonald MP (2006) Spatial and nonspatial escape strategies in the Barnes maze. *Learn Mem* 13:809–819.
32. Jones MW, Wilson MA (2005) Theta rhythms coordinate hippocampal-prefrontal interactions in a spatial memory task. *PLoS Biol* 3:e402.
33. Bowyer SM (2016) Coherence a measure of the brain networks: Past and present. *Neuropsychiatr Electrophysiol* 2:1.
34. Mitra PP, Pesaran B (1999) Analysis of dynamic brain imaging data. *Biophys J* 76:691–708.
35. Jung MW, Qin Y, McNaughton BL, Barnes CA (1998) Firing characteristics of deep layer neurons in prefrontal cortex in rats performing spatial working memory tasks. *Cereb Cortex* 8:437–450.
36. Hok V, Save E, Lenck-Santini PP, Poucet B (2005) Coding for spatial goals in the prelimbic/infralimbic area of the rat frontal cortex. *Proc Natl Acad Sci USA* 102:4602–4607.
37. Hill AJ (1978) First occurrence of hippocampal spatial firing in a new environment. *Exp Neurol* 62:282–297.
38. Frank LM, Stanley GB, Brown EN (2004) Hippocampal plasticity across multiple days of exposure to novel environments. *J Neurosci* 24:7681–7689.
39. Packard MG, McGaugh JL (1996) Inactivation of hippocampus or caudate nucleus with lidocaine differentially affects expression of place and response learning. *Neurobiol Learn Mem* 65:65–72.
40. Packard MG, McGaugh JL (1992) Double dissociation of fornix and caudate nucleus lesions on acquisition of two water maze tasks: Further evidence for multiple memory systems. *Behav Neurosci* 106:439–446.
41. Packard MG, Hirsh R, White NM (1989) Differential effects of fornix and caudate nucleus lesions on two radial maze tasks: Evidence for multiple memory systems. *J Neurosci* 9:1465–1472.
42. White NM, McDonald RJ (2002) Multiple parallel memory systems in the brain of the rat. *Neurobiol Learn Mem* 77:125–184.
43. de Bruin JP, Moita MP, de Brabander HM, Joosten RN (2001) Place and response learning of rats in a Morris water maze: Differential effects of fimbria fornix and medial prefrontal cortex lesions. *Neurobiol Learn Mem* 75:164–178.
44. Kesner RP, Farnsworth G, DiMattia BV (1989) Double dissociation of egocentric and allocentric space following medial prefrontal and parietal cortex lesions in the rat. *Behav Neurosci* 103:956–961.
45. Berke JD, Hetrick V, Breck J, Greene RW (2008) Transient 23-30 Hz oscillations in mouse hippocampus during exploration of novel environments. *Hippocampus* 18:519–529.
46. França AS, et al. (2014) Beta2 oscillations (23-30 Hz) in the mouse hippocampus during novel object recognition. *Eur J Neurosci* 40:3693–3703.
47. Kitanishi T, et al. (2015) Novelty-induced phase-locked firing to slow gamma oscillations in the hippocampus: Requirement of synaptic plasticity. *Neuron* 86:1265–1276.
48. Buschman TJ, Miller EK (2007) Top down versus bottom up control of attention in the prefrontal and posterior parietal cortices. *Science* 315:1860–1862.
49. Pesaran B, Nelson MJ, Andersen RA (2008) Free choice activates a decision circuit between frontal and parietal cortex. *Nature* 453:406–409.
50. Kopell N, Kramer MA, Malerba P, Whittington MA (2010) Are different rhythms good for different functions? *Front Hum Neurosci* 4:187.
51. Buschman TJ, Denovellis EL, Diogo C, Bullock D, Miller EK (2012) Synchronous oscillatory neural ensembles for rules in the prefrontal cortex. *Neuron* 76:838–846.
52. Engel AK, Fries P (2010) Beta-band oscillations—Signalling the status quo? *Curr Opin Neurobiol* 20:156–165.
53. Siapas AG, Lubenov EV, Wilson MA (2005) Prefrontal phase locking to hippocampal theta oscillations. *Neuron* 46:141–151.
54. Igarashi KM, Lu L, Colgin LL, Moser M-B, Moser EI (2014) Coordination of entorhinal-hippocampal ensemble activity during associative learning. *Nature* 510:143–147.
55. Spellman T, et al. (2015) Hippocampal-prefrontal input supports spatial encoding in working memory. *Nature* 522:309–314.
56. Adhikari A, Topiwala MA, Gordon JA (2011) Single units in the medial prefrontal cortex with anxiety-related firing patterns are preferentially influenced by ventral hippocampal activity. *Neuron* 71:898–910.
57. Powell NJ, Redish AD (2016) Representational changes of latent strategies in rat medial prefrontal cortex precede changes in behaviour. *Nat Commun* 7:12830.
58. Harris KD, Henze DA, Csicsvari J, Hirase H, Buzsáki G (2000) Accuracy of tetrode spike separation as determined by simultaneous intracellular and extracellular measurements. *J Neurophysiol* 84:401–414.